Proceedings of the 6th ASMO UK/ISSMO Conference on Engineering Design Optimization
(In CD-ROM), Oxford, UK, July 3-4, 2006

FINDING ROBUST SOLUTIONS TO MULTI-OBJECTIVE OPTIMISATION PROBLEMS USING POLYNOMIAL CHAOS

A. Molina-Cristobal, G. T. Parks, P. J. Clarkson

Engineering Design Centre, Department of Engineering, University of Cambridge,
Trumpington Street, Cambridge CB2 1PZ, UK.
E-mail: am664@cam.ac.uk

ABSTRACT

If an optimal solution is very sensitive to perturbations, then it may not be the most appropriate solution to use. In situations where natural variation is inevitable, it is therefore necessary to find a robust optimal solution. This paper examines emerging techniques for finding robust solutions to multi-objective optimisation problems. One of the major concerns in robust optimisation is that accounting for the robustness of solutions makes the problem much more computationally expensive. It is shown that the polynomial chaos approach addresses this key issue by decomposing the stochastic process into its deterministic and random process parts. A practical problem, design of an electrical RLC circuit, is used to illustrate the effectiveness of the approach.

Key words: multi-objective optimisation, robust design, polynomial chaos, robust optimisation.

INTRODUCTION

In evolutionary multi-objective optimisation research the main focus has been on finding the global optimum or the set of global Pareto-optimal solutions. Recently there has been growing interest in finding not only Pareto-optimal solutions, but also robust solutions (Jin and Sendhoff, 2003; Deb and Gupta, 2005; Gupta and Deb, 2005). In many real-world optimisation problems a wide range of uncertainties, such as manufacturing tolerances, noise in sensor measurements and variations in operating conditions, have to be taken into account (Bryant *et al.*, 2005; Kumar *et al.*, 2005). When design variables are subject to perturbations or changes after the optimal solution has been determined, a necessary requirement will be to establish whether the solution obtained is very sensitive to small perturbations.

Robust optimisation has been intensively studied for single-objective problems, and more recently in evolutionary multi-objective optimisation (Jin and Branke, 2005). It has been shown that one should work with a fitness function based on probability distributions of the possible perturbations, in other words, the expected fitness function (Tsutsui and Ghosh, 1997). It has been noted that an analytical closed form of the expected fitness function is not usually available; it is often approximated using Monte Carlo simulation (MCS). The most common approach has been to obtain the mean and standard deviation of the fitness function by sampling a number of points in the neighbourhood of a given solution (Branke, 1998; Deb and Gupta, 2005). However, this implies imposing additional computational cost to an optimisation problem that may well be expensive already. Here a key issue is how extensive the sampling has to be to ensure accuracy; it is well known that MCS can require a large number of samples in order to achieve accuracy.

In stochastic processes, the homogenous chaos of Wiener (1938), recently extended to generalized polynomial chaos (Xiu and Karniadakis, 2002), provides a framework for the statistical analysis of dynamic systems, at far lower computational cost than MCS. It employs Hermite polynomials in terms of Gaussian random variables. Wiener's polynomial chaos establishes that a random process with finite second-order moments can be decomposed into an infinite, convergent series of polynomials in a random variable (Wiener, 1938). It has been shown that the convergence to zero error in the mean and standard deviation is exponential as the order of the polynomial chaos increases. Therefore, truncation of the polynomial chaos can give sufficient accuracy in the computation of the mean and standard deviation for practical purposes. It is worth mentioning that polynomial chaos has been successfully applied in the fields of solid mechanics (Ghanem and Spanos, 1991), fluid dynamics (CFD) (Xiu *et al.*, 2002) and power electronics (Monti *et al.*, 2005).

This paper shows that by using the polynomial chaos approach in multi-objective optimisation it is possible

to reveal sensitive regions of the Pareto-optimal set. A benchmark electrical circuit is used for this purpose.

POLYNOMIAL CHAOS

Let us first define the terms random field, random process and random variable. A random field is a probability space, (S,$P(A)$), where S represents all possible (random) events, and $P(A)$ represents the probability of event A. A random process $X(t,\theta)$ represents a family or ensemble of functions of time t and of a random variable or random variables θ; it will be notated $X(\theta)$ for convenience. For a fixed time t, $X(\theta)$ becomes, in effect, a random variable.

The original polynomial chaos was first introduced by Wiener (1938) as homogeneous chaos. It employs Hermite polynomials in terms of a Gaussian random variable ξ. Ghanem and Spanos (1991) used the Karhunen-Loève (KL) expansion technique and homogeneous chaos to represent multiple random variables in terms of Gaussian random variables, by expanding in a series of generalised chaos polynomials. This approach was named polynomial chaos (PC). Most of physical processes are second-order random processes $X(\theta)$, viewed as a function of θ, a random event with finite variance. Applying the PC expansion, $X(\theta)$ can be represented in the form

$$X(\theta) = a_0 H_0 + \sum_{i_1=1}^{\infty} a_{i_1} H_1(\xi_{i_1}(\theta)) + \\ + \sum_{i_1=1}^{\infty} \sum_{i_2=1}^{i_1} a_{i_1 i_2} H_2(\xi_{i_1}(\theta), \xi_{i_2}(\theta)) + \cdots \quad (1)$$

where $H_n(\xi_{i_1}(\theta), ..., \xi_{i_n}(\theta))$ denotes the Hermite polynomial of order n in terms of the multi-dimensional independent standard Gaussian random variables $\boldsymbol{\xi} = (\xi_{i_1}, ..., \xi_{i_n})$ with zero means and unit variances, denoted $N[0,1]$. The general expression of the Hermite polynomials is

$$H_n(\xi_{i_1}, ..., \xi_{i_n}) = e^{\frac{1}{2}|\boldsymbol{\xi}|^2} (-1)^n \frac{\partial^n}{\partial \xi_{i_1} \cdots \partial \xi_{i_n}} e^{-\frac{1}{2}|\boldsymbol{\xi}|^2} \quad (2)$$

where $|\boldsymbol{\xi}|^2 = \sum_{i=1}^{n} \xi_{i_n}^2$. For notational convenience, equation 1 is rewritten as

$$X(\theta) = \sum_{j=0}^{\infty} \hat{a}_j \Phi_j(\boldsymbol{\xi}) \quad (3)$$

where there is a one-to-one correspondence between the functions $H_n(\xi_{i_1}(\theta), ..., \xi_{i_n}(\theta))$ and $\Phi_j(\boldsymbol{\xi})$, and also between the coefficients $\hat{a}_j$ and $a_{i_1,...,i_n}$. The polynomial basis $\Phi_j(\boldsymbol{\xi})$ of Hermite-chaos forms a complete orthogonal basis in the Hilbert space of the Gaussian random variables, i.e.

$$\langle \Phi_i \Phi_j \rangle = \langle \Phi_i^2 \rangle \delta_{ij} \quad (4)$$

where δ_{ij} is the Kronecker delta and $\langle \cdot, \cdot \rangle$ denotes the ensemble average. This is the inner product in the Hilbert space of the Gaussian random variables

$$\langle f(\boldsymbol{\xi}) g(\boldsymbol{\xi}) \rangle = \int f(\boldsymbol{\xi}) g(\boldsymbol{\xi}) W(\boldsymbol{\xi}) d\boldsymbol{\xi} \quad (5)$$

where the weighting function $W(\boldsymbol{\xi})$ is

$$W(\boldsymbol{\xi}) = \frac{1}{(2\pi)^{n/2}} e^{-\frac{1}{2}|\boldsymbol{\xi}|^2} \quad (6)$$

Note that $W(\boldsymbol{\xi})$ has the form of an n-dimensional independent Gaussian probability density function (PDF). The total number of expansion terms is $(P+1)$ and is determined by the dimension n of random variable $\boldsymbol{\xi}$ and the highest desired order p of the polynomial Φ_i,

$$(P+1) = \frac{(n+p)!}{n!p!} \quad (7)$$

It is worth mentioning that PC expansion has been extended to other probability distributions, such as Uniform, Gamma, Binomial, etc. (Xiu and Karniadakis, 2002). It is also applicable to partial differential equations (PDEs), such as the Navier-Stokes equations (Xiu *et al.*, 2002).

BENCHMARK PROBLEM

Consider a RLC (resistance-inductance-capacitance, series) electrical circuit. Using the laws of Kirchhoff, the second-order linear ordinary differential equations (ODEs) governing its behaviour are written as follows:

$$\frac{dI(t)}{dt} + \frac{R}{L} I(t) + \frac{1}{L} V_c(t) = \frac{1}{L} V_e \\ \frac{dV_c(t)}{dt} = \frac{1}{C} I(t) \quad (8)$$

where $I(t)$ is the current through the circuit, $V_c(t)$ is the voltage across the capacitor, and V_e is the source voltage.

Now, consider the stochastic problem where ($\bar{R}$, σ_R), ($\bar{L}$, σ_L), ($\bar{V}_e$, σ_{V_e}) are the mean and standard deviation of the parameters R, L, and V_e respectively; an independent Gaussian distribution is assumed, and C is set constant. When using PC expansion, a Gaussian random variable can be reduced to a linear combination of its mean and standard deviation $\alpha(\theta) = \bar{\alpha} + \sigma_\alpha \xi(\theta)$, where $\xi(\theta) \in N[0,1]$. Eq. (8) involves a combination of random variables; for notational convenience it is rewritten as

$$\frac{dI(t,\theta)}{dt} + M(\theta) I(t,\theta) + K(\theta) V_c(t,\theta) = F(\theta) \\ \frac{dV_c(t,\theta)}{dt} = \frac{1}{C} I(t,\theta) \quad (9)$$

where the parameters $M(\theta) = R(\theta)/L(\theta)$, $K(\theta) = 1/L(\theta)$ and $F(\theta) = K(\theta)V_e(\theta)$.

Exploiting the properties of operations on multiple random variables one can work out that $\bar{K} = 1/\bar{L}$, $\sigma_K = (1/\bar{L})^2\sigma_L$, $\bar{M} = \bar{R}\bar{K}$, $\sigma_M^2 = (\bar{K}\sigma_R)^2 + (\sigma_K\bar{R})^2$, and similarly for $F(\theta)$ (Peebles, 2001).

Finally, as the proposed RLC problem has three random variables, its PC expansion is written as follows:

$$\begin{aligned} M(\theta) &= \bar{M} + \sigma_M\xi_1(\theta) \\ K(\theta) &= \bar{K} + \sigma_K\xi_2(\theta) \\ F(\theta) &= \bar{F} + \sigma_F\xi_3(\theta) \end{aligned} \tag{10}$$

The PC expansion of the random process variables $V_c(t,\theta)$, $I(t,\theta)$ is expressed using a truncated expansion (Eq. (3)) as follows:

$$\begin{aligned} I(t,\theta) &= \sum_{j=0}^{P} I_j(t)\Phi_j(\boldsymbol{\xi}(\theta)) \\ V_c(t,\theta) &= \sum_{j=0}^{P} V_{cj}(t)\Phi_j(\boldsymbol{\xi}(\theta)) \end{aligned} \tag{11}$$

Notice that $\Phi_j(\boldsymbol{\xi}(\theta))$, in Eqs. (11), captures the stochastic behaviour of the dynamic system, allowing $I_j(t)$ and $V_{cj}(t)$ to be deterministic. The goal is to solve the RLC problem, Eqs. (8), using this truncated expansion, where $\boldsymbol{\xi} = (\xi_1, \xi_2, \xi_3)$ is a three-dimensional Gaussian random vector according to the random inputs. Substituting the expansion into the RLC governing equations:

$$\begin{aligned} &\sum_{k=0}^{P}\frac{dI_k}{dt}\Phi_k + \sum_{i=0}^{P}\sum_{j=0}^{P} m_i I_j \Phi_i\Phi_j + \\ &+ \sum_{i=0}^{P}\sum_{j=0}^{P} k_i V_{cj}\Phi_i\Phi_j = \sum_{k=0}^{P} f_k(t)\Phi_k \\ &\sum_{k=0}^{P}\frac{dV_{ck}}{dt}\Phi_k = \frac{1}{C}\sum_{k=0}^{P} I_k\Phi_k \end{aligned} \tag{12}$$

Employing the orthogonality relation (Eq. (4)), this system of ODEs can be simplified to:

$$\begin{aligned} \frac{dI_k}{dt} + \frac{1}{\langle\Phi_k^2\rangle}\sum_{i=0}^{P}\sum_{j=0}^{P}(m_i I_j + k_i V_{cj})e_{ijk} &= f_k(t) \\ \frac{dV_{ck}}{dt} &= \frac{1}{C}I_k \end{aligned} \tag{13}$$

This is a system of $(P+1)$ coupled ODEs. The number of ODEs needed is given by Eq. (7), where in this case $n = 3$, and p is the order of the polynomials Φ. It has been shown that $p = 3$ gives good approximations to the exact values, since PC converges to zero error exponentially (Xiu and Karniadakis, 2002). Therefore $P = 19$ here.

In the ODEs (Eqs. (13)), m_i, k_i and f_k are the coefficients of the PC expansion. In this case only the first four Hermite polynomials are needed, and these can be obtained analytically from Eq. (2): $\Phi_0 = 1$, $\Phi_1 = \xi_1$, $\Phi_2 = \xi_2$, $\Phi_3 = \xi_3$.

Then, $F(\theta) = f_0 + f_1\xi_1 + f_2\xi_2 + f_3\xi_3 + \cdots + f_P\Phi_P$, for example. By comparing this expression with $F(\theta)$ in Eq. (10), it is clear that all the coefficients are zero except $f_0 = \bar{F}$ and $f_3 = \sigma_F$. Similarly, $K(\theta) \equiv (k_0 = \bar{K},\ k_2 = \sigma_K)$ and $M(\theta) \equiv (m_0 = \bar{M},\ m_1 = \sigma_M)$.

Finally, $e_{ijk} = \langle\Phi_i, \Phi_j, \Phi_k\rangle$ can be obtained from

$$e_{ijk} = \frac{1}{(2\pi)^{n/2}}\iiint \Phi_i\Phi_j\Phi_k e^{-\frac{1}{2}(\xi_1^2+\xi_2^2+\xi_3^2)}d\xi_1 d\xi_2 d\xi_3 \tag{14}$$

Note that the Hermite polynomials $\{\Phi\}$ don't depend on the problem. $\langle\Phi_k^2\rangle$ can be computed using Eq. (14) with $j = k$ and without Φ_i. The polynomials can either be obtained using Eq. (2) or from a table in (Ghanem and Spanos, 1991).

For the case under consideration, the 20 coupled ODEs (Eqs. (13)) can be solved using any conventional method, e.g. Runge-Kutta. After finding the PC expansion coefficients, $V_{cj}(t,\theta)$ and $I_j(t,\theta)$ have the analytical forms of stochastic process solutions. Thus, the mean solution is the first term of the expansion (with an index of zero): $\bar{V}_c(t) = V_{c0}(t)$ and $\bar{I}(t) = I_0(t)$. The standard deviations of the solutions are obtained as:

$$\begin{aligned} \sigma_I^2(t) &= \langle(I(t) - \bar{I}(t))^2\rangle = \sum_{j=1}^{P}[I_j^2(t)\langle\Phi_j^2\rangle] \\ \sigma_{V_c}^2(t) &= \langle(V_c(t) - \bar{V}_c(t))^2\rangle = \sum_{j=1}^{P}[V_{cj}^2(t)\langle\Phi_j^2\rangle] \end{aligned} \tag{15}$$

The performance of the RLC system might be assessed using its step response. For a step voltage input, with mean $\bar{V}_e$ of 1V and standard deviation, σ_{V_e} of 0.1V, mean $\bar{R}$ of 1Ω and σ_R of 0.2Ω, mean $\bar{L}$ of 1H and σ_L of 0.2H, and assuming an independent Gaussian distribution, the step response when C is 1F is shown in Figure 1. Figure 1 also shows the mean and standard deviation of the step response estimated from 2000 MC simulations, and the approximations of the mean and standard deviation found using the PC approach, with the latter being obtained in a single run. It can be seen that the differences between the MCS and PC estimates of the mean and standard deviation are small, but, for this case, the computional cost of finding these using PC is approximately 200 times smaller than that for using MCS.

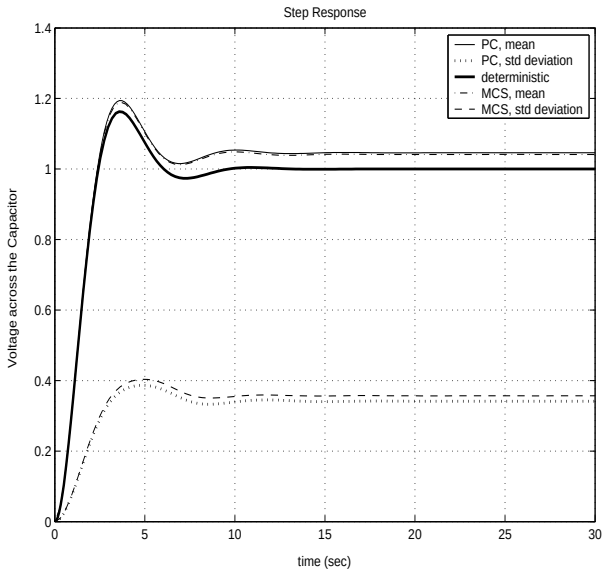

Figure 1. Step responses with Monte Carlo simulations and polynomial chaos

In the next section, we will show how PC expansion can be embedded in an evolutionary multi-objective optimisation algorithm to facilitate the identification of robust solutions.

ROBUST MULTI-OBJECTIVE OPTIMISATION

Most real-world optimisation problems, particularly in the design domain, feature multiple conflicting objectives. Thus, a trade-off exists between these objectives, which can be investigated by using multi-objective optimisation methods. In such a problem, no single optimal solution exists, rather there is a set of equally valid optimal solutions or non-dominated solutions, known as the Pareto-optimal set. The solutions in this set show the designer what is possible, allowing them to make a fully informed choice of solution.

For example, in Figure 1 one can define the overshoot, M_p, as the maximum system response relative to its final steady-state response, and the peak time, t_p, as the time it takes the system to reach this peak response. If we seek to minimise both M_p and t_p by varying R in the range [5Ω, 18Ω], with $C = 0.01$F and other values as before, there turns out to be a trade-off between M_p and t_p, as shown in Figure 2.

In Figure 2, there are two curves: the one marked with squares □ is the mean Pareto front, and the one marked with diamonds ◇ is the deterministic, or original, Pareto front. Intuitively, the robustness of a solution might be defined by how far that solution deviates from its original value in the presence of a perturbation. Using this concept, one can see that for values of M_p above 0.15V the Pareto front is robust to perturbations in R, L and input voltage V_e, while for values of M_p below 0.15V the Pareto front becomes increasingly sensitive to perturbations.

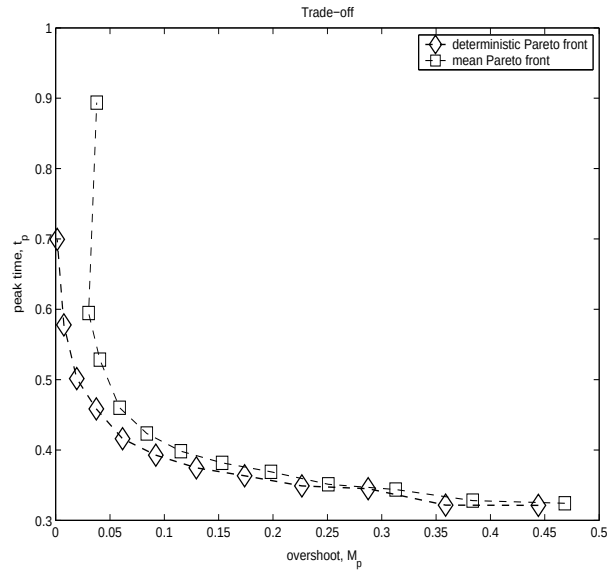

Figure 2. The Pareto front for the benchmark RLC circuit

In robust multi-objective optimisation, two approaches predominate: expectation-based search for robust solutions and expectation-variance-based measures for robustness (Jin and Sendhoff, 2003). We will examine the expectation-based approach first.

Expectation-based approach

In (Deb and Gupta, 2005) two types of multi-objective robust solutions were defined.

Type I: A solution $\boldsymbol{x}^*$ is called a multi-objective robust solution of type I, if it is the Pareto-optimal solution to the multi-objective minimisation of the mean or expected objectives defined with respect to a δ-neighbourhood. Here robustness was measured by extending the δ-neighbourhood and accuracy was controlled by the number of points in the neighbourhood.

Using the PC approach, one can see that using this method of measuring robustness with the RLC problem will necessitate changing the means and the standard deviations $R(\bar{R}, \sigma_R)$, $L(\bar{L}, \sigma_L)$, and $V_e(\bar{V}_e, \sigma_{V_e})$. In the case of the RLC problem, the means and standard deviations are information provided by the manufacturers, not parameters that can be freely varied. For this reason, this approach might not be practical for real-world problems.

It was also found that the size of the neighbourhood is important in obtaining the true robust Pareto front. However, determining the right size of the neighbourhood is computationally expensive.

In (Deb and Gupta, 2005), a second type of multi-objective robust solution was defined: For a minimisation problem, a solution $\boldsymbol{x}^*$ is called a robust solution of type II, if it is the Pareto-optimal solution to the following problem:

$$
\begin{aligned}
&min(f_1(\boldsymbol{x}), f_2(\boldsymbol{x}), \ldots, f_n(\boldsymbol{x})) \\
&subject\ to\ \|\bar{\boldsymbol{f}}(\boldsymbol{x}) - \boldsymbol{f}(\boldsymbol{x})\| < \nu \\
&\boldsymbol{x} \in \Xi
\end{aligned} \tag{16}
$$

where the constraint $\|\bar{\boldsymbol{f}}(\boldsymbol{x}) - \boldsymbol{f}(\boldsymbol{x})\| < \nu$ is on the Euclidian distance between the mean and the deterministic objectives. This constraint can be modified according to the needs of the problem; for instance, the designer might need different values of ν_i, i=1,2,...,n, for each objective.

The type II approach, with PC being used to estimate the mean objectives, was implemented within a multi-objective evolutionary algorithm (MOEA), in particular within the multi-objective genetic algorithm (MOGA) proposed in (Fonseca and Fleming, 1998). Note that the PC-based method could be implemented with any MOEA or meta-heuristic optimisation approach.

The settings for the MOGA were: binary resolution of 32-bit Gray coding with exponential scaling in each of the variables; mating restriction; single-point crossover with probability 0.7; a mutation rate of 0.0073; and a population size of 100.

The multi-objective problem solved was:

$$
\begin{aligned}
&min(M_p(\bar{R}, \bar{L}, C), t_p(\bar{R}, \bar{L}, C)) \\
&subject\ to\ \|(\bar{M}_p, \bar{t}_p) - (M_p, t_p)\| < \nu
\end{aligned} \tag{17}
$$

where $\bar{M}_p$ is the step response overshoot from $\bar{V}_c(t)$ relative to $\bar{V}_e$, and $\bar{t}_p$ is the time to reach the peak of $\bar{V}_c(t)$. The lower and upper bounds on the decision vector $(\bar{R}, \bar{L}, C)$ were [0.5, 1, 0.01] and [30, 30, 30], respectively. The optimisation result after 100 generations is presented in Figure 3.

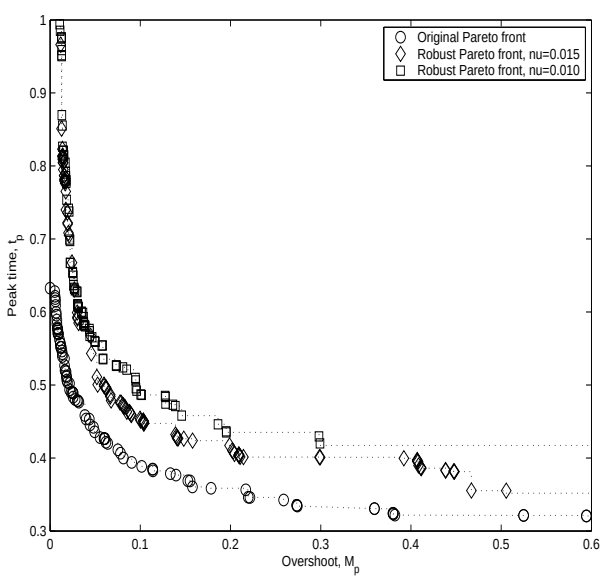

Figure 3. Robust Pareto fronts: expectation-based search for robust solutions

In Figure 3, there are three curves: the one marked with circles is the Pareto front without the constraint, in other words the Pareto-optimal set if no consideration is given to the robustness of the solutions (notice that it is similar to the deterministic Pareto front obtained in Figure 2); the curves marked with diamonds and squares are robust Pareto fronts for robustness measures of $\nu = 0.015$ and $\nu = 0.010$, respectively. Although the overall performance of the robust Pareto fronts recedes, as expected, with respect to the deterministic or original front, there is a guarantee that its Euclidian distance to the mean step response will be no greater than ν. Another characteristic that can be observed is that the Pareto front shrinks as ν decreases and increasingly robust performance is demanded. This because part of the original Pareto front is no longer non-dominated (Deb and Gupta, 2005).

Expectation-variance-based approach

It has been argued that the expectation-based approach does not adequately take into account perturbations of the objective function, and at the same time a purely variance-based measure of robustness does not take into account the absolute performance of the solution. The mean and the variance of the objective functions are, in fact, conflicting objectives, and therefore their optimisation should be treated as a multi-objective problem.

Three examples of this approach in practical engineering problems are:

- In (Bryant *et al.*, 2005), for the minimisation of the power losses in IGBT-diodes, operating conditions are taken into account, and, in order to avoid misleading selection of optimal values across the operating conditions, the minimisation of both mean and variance of power losses was considered.
- In (Kumar *et al.*, 2005), for the minimisation of the pressure losses in a turbomachinery blade with 2D CFD models, the expected-variance-based approach is used to take into account uncertainty in variables due to factors such as erosion of the blade. Here the minimisation of the mean and variance of the pressure losses was implemented. In this investigation the expected-variance-based approach was motivated from the Taguchi's method, e.g. in (Kunjur and Krishnamurty, 1997), where the Pareto-optimal robust solutions are identified with the aid of analysis of variance (ANOVA).
- In (Jin and Sendhoff, 2003), an evolutionary multi-objective approach was used to find the trade-off between the mean (performance) and the variance (robustness). One approach taken is to approximate the mean and the variance of the

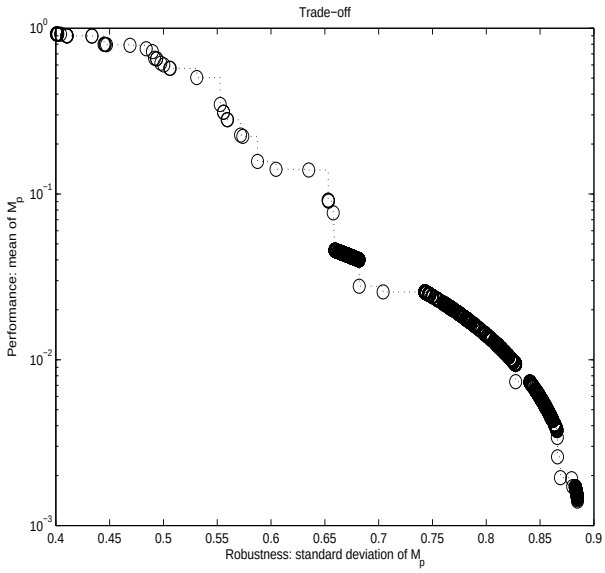

Figure 4. The trade-off between expected performance and variance

objective function using Taylor series expansions about the mean values of the decision point. A second approach used is to estimate the mean and the variance of the objective function using the current population, controlling the distance between members.

However, this approach has an obvious problem: manufacturing tolerances usually follow a specific PDF, which might well not be the same distribution as that in the current neighbourhood, in the optimisation.

Without exception, all these approaches have difficulties associated with the size of the neighbourhood and/or the computational expense in measuring robustness. The PC expansion approach might overcome these difficulties.

For the case of our RLC problem, the following multi-objective optimisation problem was solved:

$$min(\bar{M}_p(\bar{R},\bar{L},C),\sigma_{M_p}(\bar{R},\bar{L},C)) \tag{18}$$

where $\sigma_{M_p} = \sigma_{V_c}(\bar{t}_p) - 1$. The afore-mentioned MOGA settings where used again.

The optimisation result after 100 generations is presented in Figure 4. The curve marked with circles is the trade-off between robustness and performance. One can see, in the extremes of the Pareto front, that high performance means greater sensitivity to perturbations and vice versa.

Another possible approach is to combine all the performance and robustness measures in the following multi-objective optimisation problem:

$$\begin{aligned} &min(\bar{M}_p(\bar{R},\bar{L},C),\bar{t}_p(\bar{R},\bar{L},C),\sigma_{M_p}(\bar{R},\bar{L},C)) \\ &\qquad subject\ to\ \|(\bar{M}_p,\bar{t}_p)-(M_p,t_p)\| < \nu \end{aligned} \tag{19}$$

The afore-mentioned MOGA settings where used again.

The optimisation result after 100 generations, for the case $\nu = 0.015$, is presented in Figure 5. The Pareto front is the combination of the convex Pareto front from Figure 3 and the concave Pareto front from Figure 4.

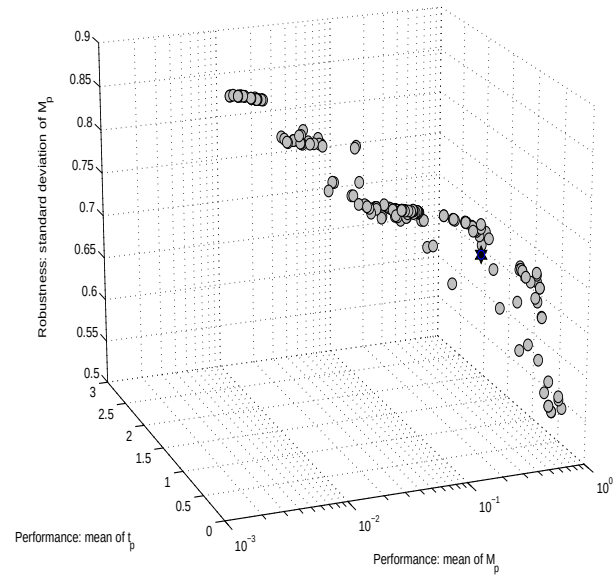

Figure 5. Robust Pareto front: variance-expectation-based search for robust solutions

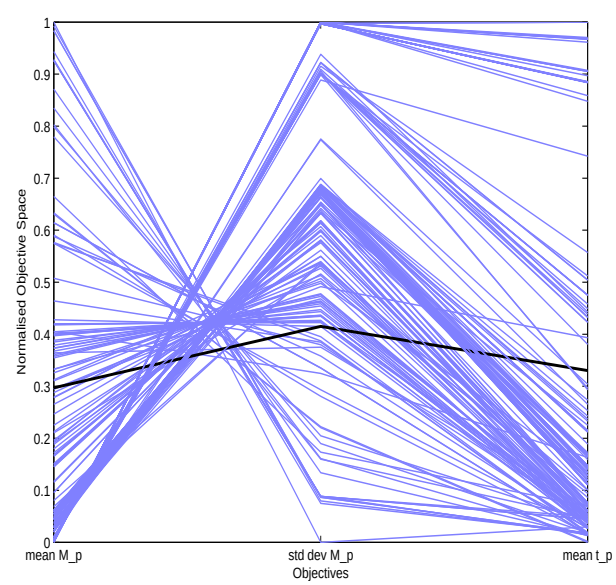

Figure 6. Parallel coordinates representation of the robust Pareto front in Figure 5

The result of a multi-objective optimisation is a Pareto front – a set of competing solutions. However, a real-life design problem will ultimately require a single solution. Assuming that the RCL circuit design problem considered here requires a solution representing the best compromise between the performance measures and the robustness measure, parallel coordinates can be used to visualise and identify such a solution, as in Figure 6.

In Figure 6 each line joining the three objectives represents a solution. The x-axis represents the objectives and the y-axis shows normalized performance in the interval $[0, 1]$. Crossing lines represent conflicting objectives. The best compromise design will be the one closest to a horizontal line across the three objectives and simultaneously with the minimum performance measure for the three objectives. The best choice for this RLC circuit design problem is indicated with a black line, and marked with a ★ in Figure 5. The values of this circuit are $C = 0.042921$F, $R = 4.3214\Omega$, and $L = 1.3645$H, and its performance and robustness measures are M_p=0.27117V, t_p=0.83683sec, $\bar{M}_p$=0.28451V, $\bar{t_p}$=0.84245sec, σ_{M_p}=0.70905V, and ν=0.014469.

CONCLUSIONS

Emerging techniques for estimating robustness have been examined in this paper. It was shown that the PC expansion approach offers a means of handling uncertainties better suited to the practicalities of real-world design problems than other existing approaches to measuring robustness. The PC expansion approach was illustrated through its application to the optimisation of a simple stochastic RLC circuit. It was shown that the PC approach effectively overcomes the issue of expensive computation of the neighbourhood when searching for robust solutions. Three approaches to finding robust solutions of multi-objective optimisation problems (the expectation-based approach, the expectation-variance-approach, and a combination of these) were presented.

Potential limitations of the PC approach are that, although the PC expansion can be truncated, the number of equations to be solved for the stochastic model increases exponentially with the number of random variables (sources of uncertainty or variability), and that it can only be used when the system to be analysed is modeled by ODEs or PDEs – though, of course, many real-world systems can be modeled by these means.

REFERENCES

Branke, J. (1998). Creating robust solutions by means of evolutionary algorithms. In: *PPSN V, LNCS 1498* (A. E. Eiben et al, Ed.). pp. 119–128. Springer-Verlag. Berlin Heidelberg.

Bryant, A.T., D.M. Jaeggi, G.T. Parks and P.R. Palmer (2005). The influence of operating conditions on multi-objective optimization of power electronic devices and circuits. In: *IEEE Industry Applications Society (IAS 2005)*. Hong Kong, China.

Deb, K. and H. Gupta (2005). Searching for robust pareto-optimal solutions in multi-objective optimization. In: *Evolutionary Multi-Criterion Optimization* ser. LNCS 3410. Springer-Verlag pp. 150–164.

Fonseca, C. M. and P. J. Fleming (1998). Multi-objective optimization and multiple constraint handling with evolutionary algorithms. I: A unified formulation. *IEEE Transactions on Systems, Man and Cybernetics-Part A: systems and humans* **28**(1), 26–37.

Ghanem, R. and P. Spanos (1991). *Stochastic Finite Elements: A Spectral Approach,* .. Springer-Verlag. N.Y.

Gupta, H. and K. Deb (2005). Handling constraints in robust multi-objective optimization. In: *IEEE Congress on Evolutionary Computation (CEC-2005)*. Edinburgh, U. K.

Jin, Y. and B. Sendhoff (2003). Trade-off between performance and robustness: An evolutionary multiobjective approach. In: *Evolutionary Multi-Criterion Optimization* ser. LNCS. Vol. 2632. Springer-Verlag. pp. 237 – 251.

Jin, Y. and J. Branke (2005). Evolutionary optimization in uncertain environments-a survey. *IEEE Transactions on Evolutionary Computation* **9**(3), 303–317.

Kumar, A., A. J. Keane, P. B. Nair and S. Shahpar (2005). Efficient genetic algorithm based robust design method for compressor fan blades. In: *2005 ASME International Design Engineering Technical Conference and Computer and Informatics in Engineering Conference*. Long Beach, California, USA, September 24-28, 2005.

Kunjur, A and S Krishnamurty (1997). A robust mult-objective optimization approach. *Mech. Mach. Theory* **32**(7), 797–810.

Monti, A., F. Ponci, T. Lovett, A. Smith and R. Dougal (2005). Modeling of uncertainty and applications in monitoring and control of power electronics. In: *Proceedings of the American Control Conference*. Vol. 3. Portland, Oregon. pp. 2011 – 2016.

Peebles, P. Z. (2001). *Probability, random variables and random signal principles*. Series in electrical and computer engineering. 4th ed.. McGraw-Hill. Boston, MA.

Tsutsui, S. and A. Ghosh (1997). Genetic algorithms with a robust solution searching scheme. *IEEE Transactions on Evolutionary Computation* **1**(3), 201–208.

Wiener, N. (1938). The homogeneous chaos. *American Journal of Mathematics* **60**(4), 897–936.

Xiu, D. and G. Em Karniadakis (2002). The wiener–askey polynomial chaos for stochastic differential equations. *SIAM Society for Industrial and Applied Mathematics* **24**(2), 619–644.

Xiu, D., D. Lucor, C.-H. Su and George Em Karniadakis (2002). Stochastic modeling of flow-structure interaction using generalized pynomial chaos. *Journa of Fluids Engineering* **124**, 51–59.